Seasonal variations in daily patterns of the quantum yield of fluorescence

Yannick Huot[1] and David Antoine[2]

1. Université de Sherbrooke, Québec, Canada

2. Curtin University, Perth, Australia & Sorbonne Universités, UPMC Univ Paris 06, INSU-CNRS, Laboratoire d'Océanographie de Villefranche, France, France

Read only the green text for a quick overview…

Introduction

The quantum yield of chlorophyll fluorescence, Φ_f, is estimated in situ or remotely using algorithms based on measurements of emitted fluorescence and estimates of the light absorbed by phytoplankton. While Sun-synchronous satellites provide global fields of Φ_f (Behrenfeld et al. 2009; Huot et al. 2013) and geostationary satellites provide time-resolved estimates (O'Malley et al. 2014), the interpretation of such measurements remains a challenge.

Here, we analyze Sun-induced fluorescence at the BOUSSOLE mooring (Ligurian Sea), which was compared with MODIS-derived estimates.

Methods

MODIS dataset: From **MODIS-Aqua level 2 data from 2010 to 2016,** averages of 5x5 pixels centered on BOUSSOLE were computed for [Chl], nflh and Φ_f (Behrenfeld et al. (2009) and Huot et al. (2013) algorithms).

BOUSSOLE dataset: The BOUSSOLE mooring measures the spectral downwelling irradiance (E_d) and upwelling radiance (L_u, μW cm^{-2} nm^{-1} sr^{-1}) at 4 m and 9 m; only the 4-m data are shown. The upwelling fluorescence radiance (L_{uf}) was separated from the total upwelling radiance at 681 nm and normalized to E_d at 490 nm ($E_d(490)$, μW cm^{-2} nm^{-1}): F (sr^{-1}). Data collected every 15 minutes were split into morning and afternoon, and fit separately using the model described below; the average of the two fits is reported.

The Fluorescence Model

F is modeled with 6 parameters as the product of two functions (e.g. Morrison 2003; Schallenberg et al. 2008): 1) f_{PQ} representing the effect of basal fluorescence and photochemical quenching, and 2) f_{NPQ} representing the effect of non-photochemical quenching, $F=f_{PQ}f_{NPQ}$. The data are fitted as a function of $E_d(490)$. We assume that an irradiance above which NPQ is initiated exists (E_{d0NPQ} , μW cm^{-2} nm^{-1}). Below and above E_{d0NPQ}, the fluorescence response of both f_{PQ} and f_{NPQ} are treated differently. For f_{NPQ} 1) we define the non-photochemical quenching amplitude (A_{NPQ}), which has values between 0 (for no quenching) and 1 (for complete quenching); and 2) a "saturation irradiance for NPQ" (E_{kNPQ}, μW cm^{-2} nm^{-1}) that is an irradiance value above which maximum fluorescence has decreased by 63%, essentially. Minimum (F_{min}) and maximum (F_{max}) values are fitted to the measured F values as well as a parameter representing the saturation of fluorescence at low light (E_{kPQ}).

$E_d(490) \geq E_{d0NPQ}$

$$f_{PQ} = F_{min} + \left(F_{max} - F_{min}\right)\left(1 - e^{\left(-E_{d0NPQ}/E_{kPQ}\right)}\right) \qquad f_{NPQ} = 1 - A_{NPQ}\left(1 - e^{\left(-\left[E_d(490) - E_{d0NPQ}\right]/E_{kNPQ}\right)} \Big/ 1 - e^{\left(-\left[E_{d\max}(490) - E_{d0NPQ}\right]/E_{kNPQ}\right)}\right)$$

$E_d(490) < E_{d0NPQ}$

$$f_{PQ} = F_{min} + \left(F_{max} - F_{min}\right)\left(1 - e^{\left(-E_d(490)/E_{kPQ}\right)}\right) \qquad f_{NPQ} = 1$$

We also computed the fluorescence value at midday (F_{noon}) for comparison with MODIS AQUA.

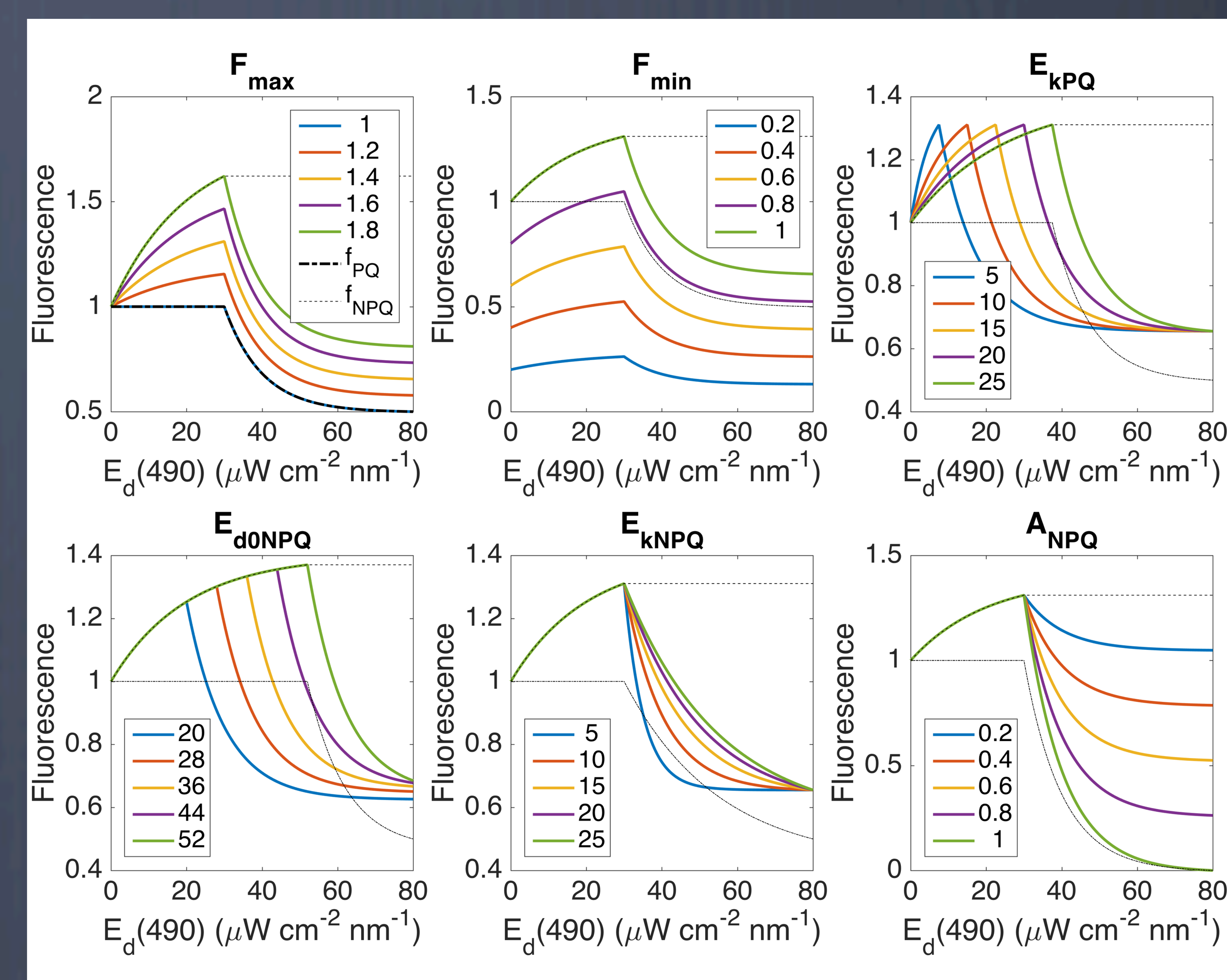

Figure 1. Effect of changing the different variables in the fluorescence model. A standard run was performed with the following variables: F_{min}=1; F_{max}=1.4; E_{kPQ}= 20 μW cm^{-2} nm^{-1}; E_{d0NPQ}=1.5E_{kPQ} μW cm^{-2} nm^{-1}; E_{kNPQ}= 10 μW cm^{-2} nm^{-1}; A_{NPQ}=0.5. For each panel, the title's variable was modified according to the values provided in the legend. In each panel, the functions f_{PQ} (dashed dotted line) and f_{NPQ} (dashed line) for the corresponding green line in the panel are provided as a reference.

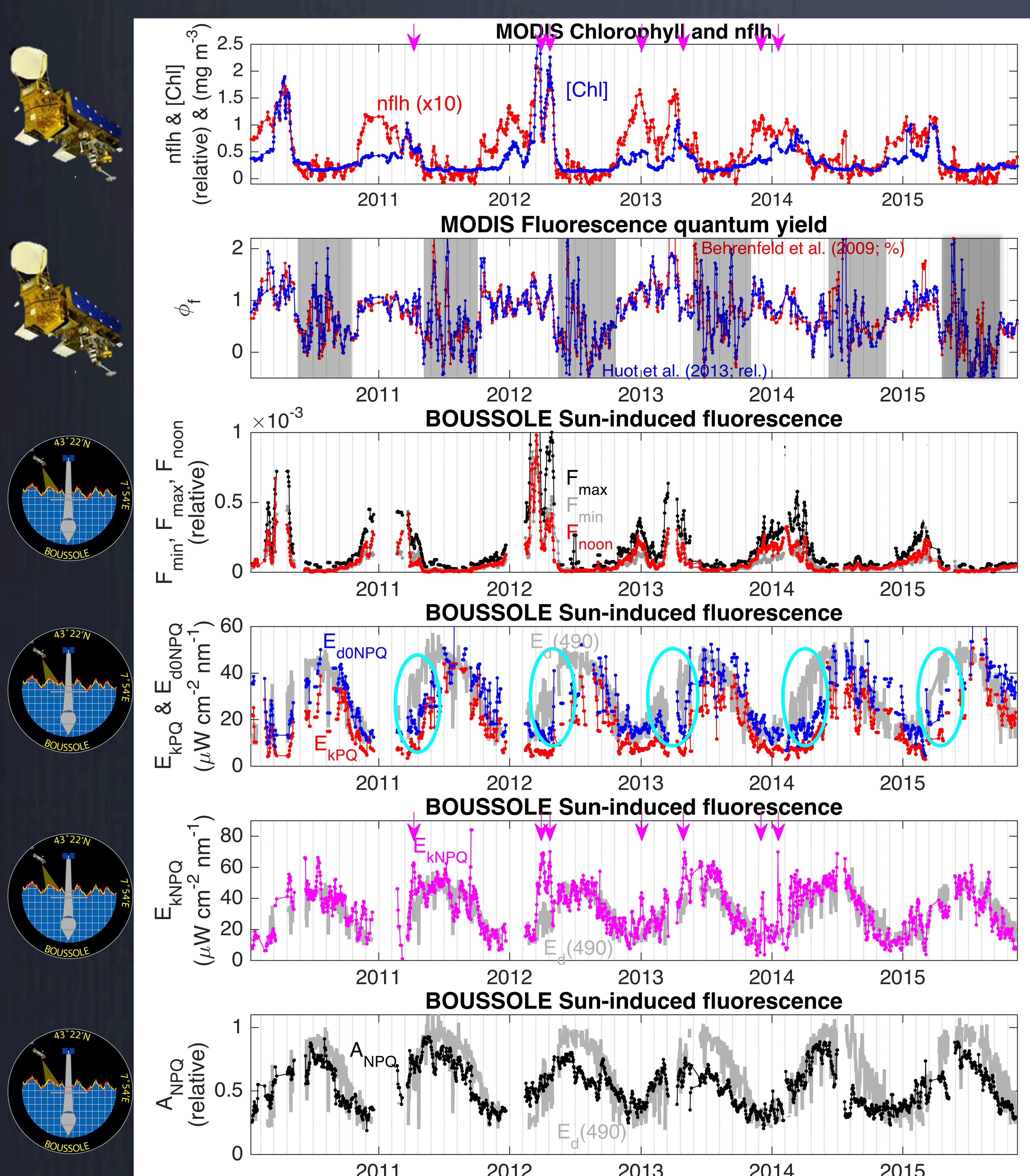

Results

Figure 2. The nflh and [Chl] follow similar annual patterns. A fall bloom, which often lasts into the winter, is followed by a spring bloom; the summer season is oligotropic. Note that nflh is the fluorescence radiance normalized by the irradiance in the same band (a "fluorescence reflectance"). As such, it is dependent on the phytoplankton absorption, the quantum yield and the attenuation coefficient.

The Φ_f was estimated by two algorithms, which both showed very similar patterns. The summer period (shaded) tends to be much more variable despite relatively constant estimates of chlorophyll. This arises from variability in the nflh (some is artifactual or noise). The bloom periods tend to show higher Φ_f; short term variability during this period appears to reflect real changes in Φ_f.

The minimum, maximum and noontime fluorescence measurements follow the MODIS nflh measurements. Depending on the time of year, the F_{noon} measurement is either above or below F_{min}.

Two variables, E_{kPQ} and E_{d0NPQ}, show very similar temporal patterns. These patterns generally follow the incident irradiance at 4 m (gray line), except during the spring bloom (highlighted with turquoise ellipses) when both variables remain low while the irradiance increases. Just after the end of the spring bloom, both variables increase rapidly. The fitting procedure forces E_{d0NPQ} to be equal or greater than E_{kPQ}. Higher E_{kPQ} is consistent with acclimation/adaptation to growth irradiance.

Variations in E_{kNPQ} very closely follow $E_d(490)$ (gray line). When irradiance is higher, the value increases, which means that quenching is less sensitive to irradiance (see Fig. 1). This is consistent with acclimation/adaptation to high light. Some high values are observed, as noted with the magenta arrows. The timing of these arrows is indicated in the top panel, which shows that these high values tend to be followed by a strong decrease in [Chl].

The relative amplitude of non-photochemical quenching also roughly follows $E_d(490)$; however, depending on the year, large and lengthy excursions from these expected trends do occur, in particular, during the summer and fall periods. As such, it is clear that other drivers of this signal exist.

Conclusions

After individually examining the different parameters that influence the shape of the fluorescence vs irradiance curve, **none of the parameters were found to explain the variability in the remotely sensed Φ_f.** Current algorithms are designed to remove much of the average effect of the incident irradiance on the quantum yield. By doing so, it is possible that the parameters obtained here, which are to different extents correlated with the incident irradiance, do not impact the variability in the remotely sensed quantum yield using current algorithms. This suggests that the **variability at the BOUSSOLE site observed in the remotely sensed Φ_f is not strongly driven by the incident (and growth) irradiance** and photoacclimation or photoadaptation processes. Our analysis also reveals important differences in the temporal changes of different parameters describing the fluorescence vs irradiance curve. In particular, **the "NPQ" part of the curve responds differently from the "PQ" part of the curve.**

References

1) Huot, Y., B.A. Franz, and M. Fradette. 2013. Estimating variability in the quantum yield of Sun-induced chlorophyll fluorescence: A global analysis of oceanic waters. Remote Sensing of Environment **132**: 238-253- .

2) O'Malley, R. T., M.J. Behrenfeld, T.K. Westberry, A.J. Milligan, S. Shang, and J. Yan. 2014. Geostationary satellite observations of dynamic phytoplankton photophysiology. Geophysical Research Letters **41**: 5052-505

3) Morrison, J. R. 2003. In situ determination of the quantum yield of phytoplankton chlorophyll a fluorescence: a simple algorithm, observations, and a model. Limnol Oceanogr **48**: 618-63

4) Schallenberg, C., M.R. Lewis, D.E. Kelley, and J.J. Cullen. 2008. The inferred influence of nutrient availability on the relationship between sun-induced fluorescence and incident irradiance in the Bering Sea. Journal of Geophysical Research **113**: C0704

Aknowledgments:

We thank the Laboratoire oceanographique deVillefranche, the Obervatoire Océanologie de Villefranche, the European Space Agency, and the Centre National d'Études Spatialesfor supporting the BOUSSOLE program as well as Curtin University, NSERC and the Canada research chair program for supporting our research.